

Numerical investigations on the along-wind response of a vibrating fence under wind action

Fuh-Min Fang[†]

Department of Civil Engineering, National Chung-Hsing University, 250 Kuo-Kuang Road, Taichung, Taiwan 40227, R.O.C.

Jin-Min Ueng[‡] and J. C. Chen^{††}

Department of Civil Engineering, National Chung-Hsing University, Taiwan, R.O.C.

Abstract. The along-wind response of a surface-mounted elastic fence under the action of wind was investigated numerically. In the computations, two sets of equations, one for the simulation of the unsteady turbulent flow and the other for the calculation of the dynamic motion of the fence, were solved alternatively. The resulting time-series tip response of the fence as well as the flow fields were analyzed to examine the dynamic behaviors of the two. Results show that the flow is unsteady and is dominated by two frequencies: one relates to the shear layer vortices and the other one is subject to vortex shedding. The resulting unsteady wind load causes the fence to vibrate. The tip deflection of the fence is periodic and is symmetric to an equilibrium position, corresponding to the average load. Although the along-wind aerodynamic effect is not significant, the fluctuating quantities of the tip deflection, velocity and acceleration are enhanced as the fundamental frequency of the fence is near the vortex or shedding frequency of the flow due to the occurrence of resonance. In addition, when the fence is relatively soft, higher mode response can be excited, leading to significant increases of the variations of the tip velocity and acceleration.

Key words: large-eddy simulation; flow-induced vibration.

1. Introduction

The interaction between an elastic structure and its surrounding flow has been an interesting subject in building research. In many studies, the aeroelastic behaviour of a vibrating body in a wind field was investigated experimentally to obtain additional insight into the dynamics of flow-induced vibration. Physically, when a flow passes a blunt body, separation usually occurs at the sharp edges. Due to shear-flow instability, vortices may be generated downstream and lead to an unsteady flow pattern. For a surface-mounted slender structure, the resulting unsteady load can cause structural vibration. If the motion is significant, the relative motion of the structure with respect to the flow can induce a change of the load distribution and further affect the structure response. This secondary effect, so-called “aerodynamic damping”, is considered important in the analysis of the wind effect on structures.

[†] Professor

[‡] Associate Professor

^{††} Research Assistant

2. Problem description

A numerical method is developed to explore the mechanisms of interaction between a vibrating structure and its surrounding flow in time domain. In particular, a problem of flow past a surface-mounted elastic fence is selected. By varying the fundamental frequency of the fence, the flow fields as well as the along-wind response of the fence are examined.

The numerical computations are carried out under a flow condition depicted in Fig. 1. The fence height (H) is 40 m. The approaching flow velocity profile, which is set at the section with a distance of $6H$ upstream the fence, is of the type of one-to-seven power-law distribution with an edge velocity of U_o (40 m/s) and a boundary layer thickness (δ) of $7H$. The corresponding Reynolds number ($Re = U_o H / \nu$; ν being the kinematic viscosity of air) is equal to 1.1×10^8 . The elastic fence is made of steel, with a Young's modulus of 200×10^9 N/m² and two selected values of modal damping ratios ($\zeta_{1,2} = 2\%$ and 5% respectively) for the first two modes. The thickness of the fence varies from 0.05 to 0.47 m, corresponding to reduced velocities ($U_r = U_o / (f_1 H)$), f_1 being the fundamental frequency of the fence) varying from 38 to 4.

3. Numerical method

The simulations contain two parts of dynamic computations, which are performed alternatively during the calculation process. To predict the unsteady turbulent flow around the fence, a weakly-compressible-flow method (Song and Yuan 1988), together with the Smagorinsky subgrid-scale turbulence model (Smagorinsky 1963) is adopted. In the second part of the calculations, the fence structure is treated as a linear, multi-degree-of-freedom system with proportional damping. For each fence element, the axial force is neglected, and the net wind force is converted to an equivalent lateral force and bending moment (see Fig. 2) based on a consistent approach. The history of the fence response is calculated based on the mode superposition method.

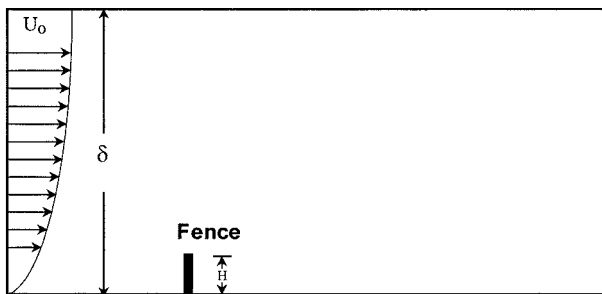


Fig. 1 Sketch of the problem

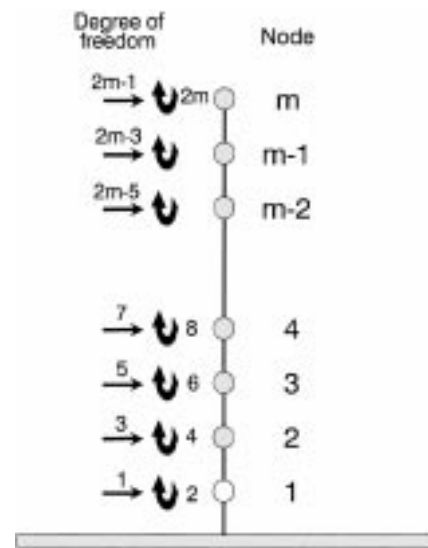


Fig. 2 Sketch of the MDOF fence system

After an instantaneous flow field is simulated, the pressure distribution along the fence is taken as an input to calculate the structural response. The resulting deflection and the vibration speed of the fence are then fed back to the boundary specifications of the fence for the flow calculation in the following time step. The alternative solutions of the instantaneous flow field and the along-wind fence response are considered the results of the interactive dynamic behaviors of the two.

4. Results

4.1. Flow field without interaction

An initial calculation is performed to simulate the flow as the fence is rigid ($U_r = 0$). Figs. 3 illustrate the history of the normalized vorticity field {defined as $\Omega = H / U_o(\partial \bar{v} / \partial x - \partial \bar{u} / \partial y)$ }, around the fence within a typical period. A process of vortex formation and detachment is clearly detected. The history of the drag coefficient ($C_D = 2F_D / \rho U_o^2 H$, F_D being the drag force per unit width of the fence) in Fig. 4 also indicates the unsteady feature of the flow. Two peak values are detected in the spectrum of the drag coefficient (Fig. 5). The corresponding Strouhal numbers { $St = (fH / U_o)$, f being the dominant frequency of the flow} are respectively 0.0323 and 0.0606.

4.2. Tip response of the fence

By varying the reduced velocity, it is found in all cases that the tip deflects periodically. Figs. 6 illustrate a typical example of the tip history of the response as U_r and $\zeta_{1,2}$ are equal to 12 and 2%,

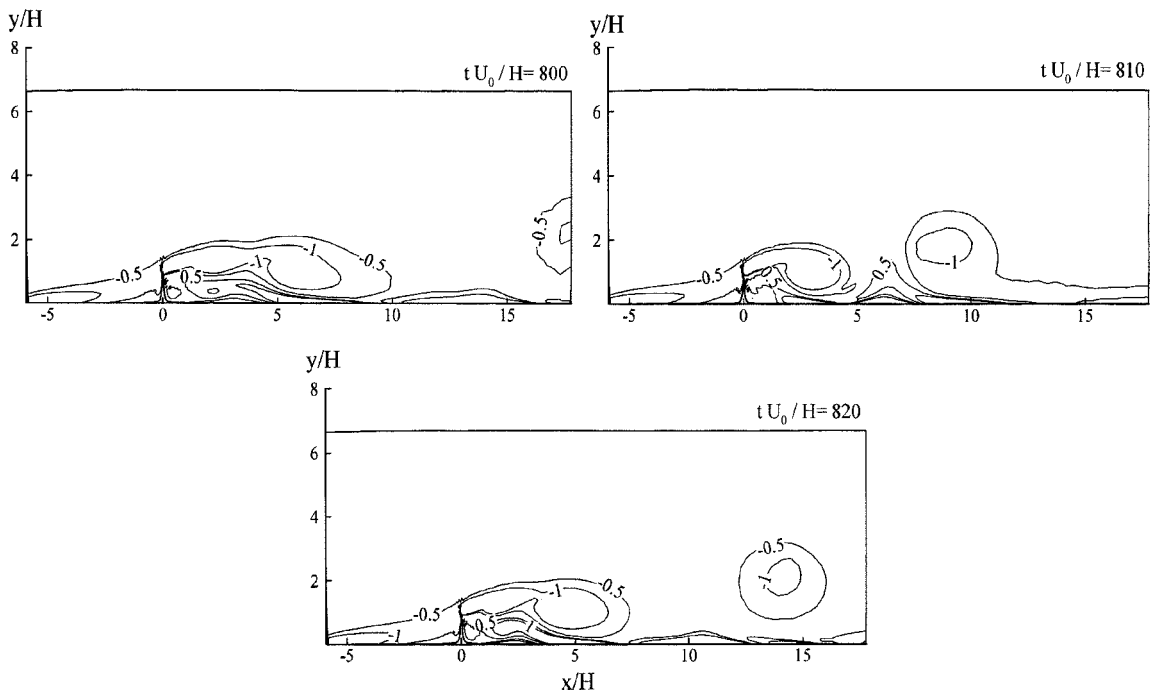


Fig. 3 Normalized vorticity fields at three instants

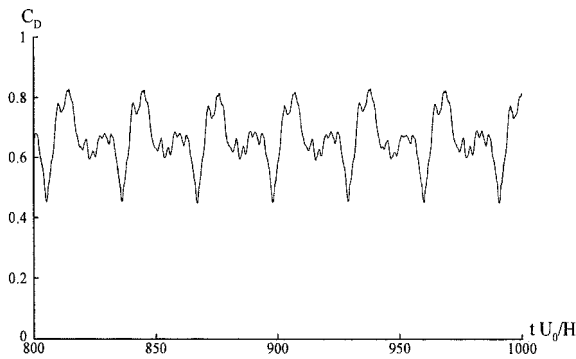


Fig. 4 History of drag coefficient

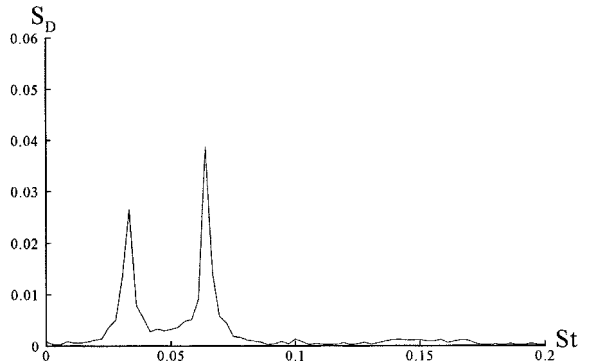


Fig. 5 Power spectrum of drag coefficient

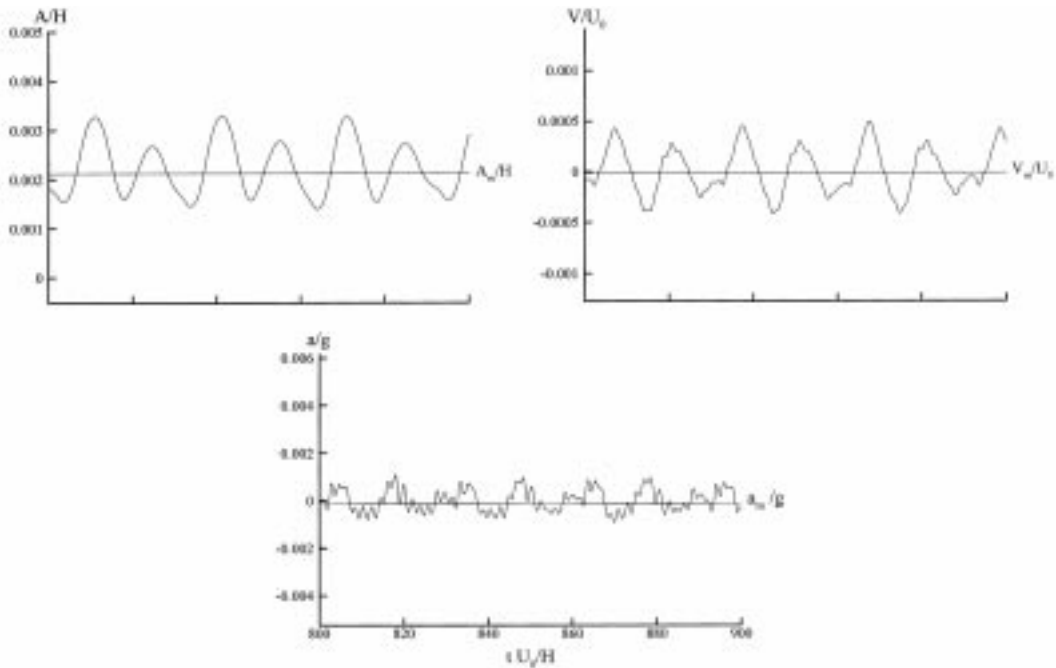


Fig. 6 Tip response histories ($U_r = 12$, $\zeta_{1,2} = 2\%$)

where A , V and a represent respectively the tip deflection, velocity and acceleration of the vibrating fence. As the tip deflection is at a maximum or minimum value, the instantaneous tip speed is zero. Meanwhile, the corresponding tip acceleration reaches a maximum level but is in an opposite direction.

Figs. 7 depict the average values of the tip deflection (A_m), velocity (V_m) and accelerations (a_m) with the two modal damping ratios at various reduced velocities. As U_r increases, the mean tip deflection of the fence also increases (Fig. 7a). Since the tip vibrates symmetrically, the mean tip velocities (V_m) and accelerations (a_m) in all cases are nearly zero (Figs. 7b and 7c). Additionally, the variation of modal damping ratio does not appear to affect all the mean quantities.

As the variations of the tip response are concerned, calculated results (Figs. 8) show that the modal damping ratio play an important role in affecting the root-mean-square values of the tip deflection (A_r),

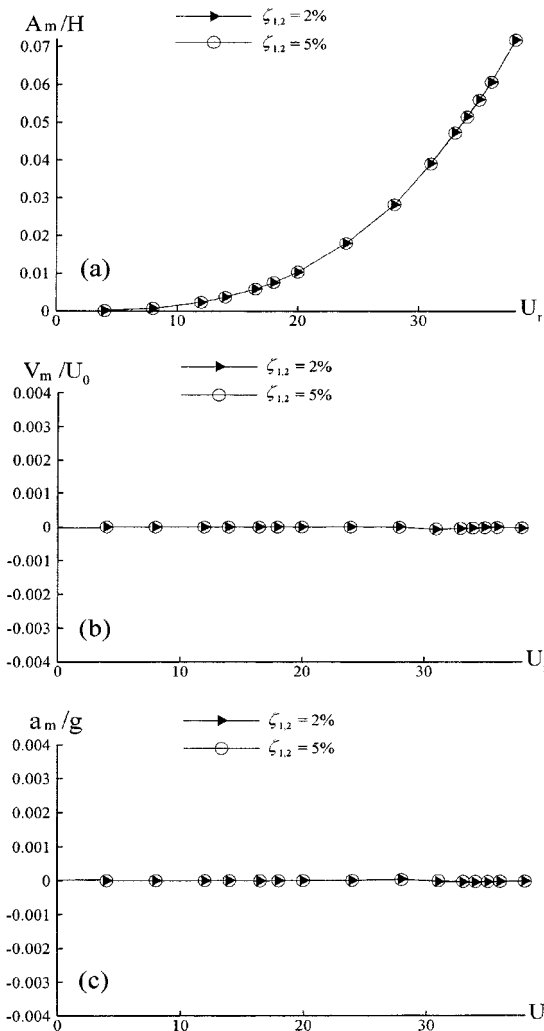


Fig. 7 Mean quantities of tip response at various reduced velocities

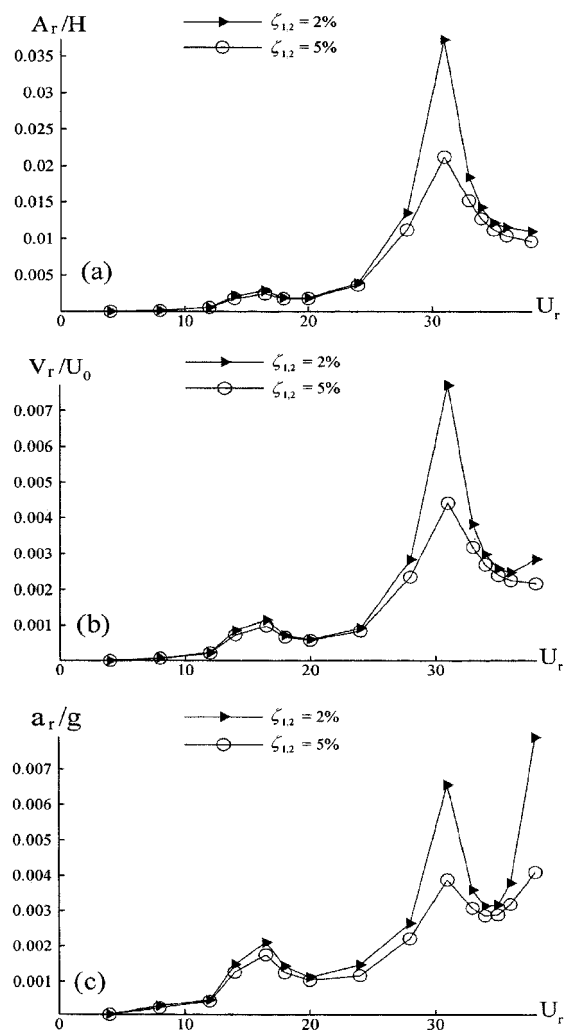


Fig. 8 Root-mean-square quantities of tip response at various reduced velocities

velocity (V_r) and acceleration (a_r), especially when resonance occurs or when the fence becomes relatively soft ($U_r > 35$). In the case that the fundamental frequency of the fence (f_1) is equal to the most dominant vortex frequency (or when $U_r = 16.5$, being the reciprocal of the Strouhal number corresponding to 0.0606), peak values of A_r , V_r and a_r are obtained. As the reduced velocity increases, the fluctuating quantities start to decrease until U_r reaches a value of about 20. After that, more significant peak values of the fluctuating quantities are obtained when f_1 is near the shedding frequency (or when $U_r = 31$, being the reciprocal of the Strouhal number equal to 0.0323). After U_r exceeds about 35, A_r remains a trend of decrease; so does the trend of V_r in the case with a greater value of modal damping ($\zeta_{1,2} = 5\%$). Within the same range of U_r , however, tendencies of dramatic increases are obtained for a_r , and for V_r in the case with a smaller value of modal damping ($\zeta_{1,2} = 2\%$).

5. Discussion

Though the problem case may be somewhat impractical, the outcome from the numerical results is considered fruitful. By combining two sets of solvers, the numerical model is applicable to predict the dynamic behaviors of the flow and the vibrating fence in time series, and allows for detailed examinations on the vibration mechanisms.

As wind passes the fence, vortices are generated and then produce flow unsteadiness. Two dominant frequencies are found: one related to the shear layer vortices and the other one subject to vortex shedding. As the spectrum of C_D (Fig. 5) is examined, the peak corresponding to $St = 0.0606$ appears more significant. The unsteady flow pattern has been monitored by Fang *et al.* (1997) in a water tunnel, and the correctness of the numerical results, such as the mean velocity profiles at various cross-sections of the flow field, has been confirmed by comparing with the experimental data from Gupta *et al.* (1987). For a uniform flow past a normal solid fence in an open flow field at a Reynolds number of 10^4 , the Strouhal number is about 0.14 (Pearce, Qasim, Maxwell and Parameaswaran 1992), while in the present case the corresponding value is about one-half. The reason, as explained by Fang *et al.* (1997), is due to the fact that the former involves merging of vortices from both sides of the fence tips and there is no vortex merging in the latter case. Additional results (Fang, Hsieh, Jong and She 1997) also show that the normalized flow field becomes independent of the Reynolds number as Re exceeds about 10^5 . Further investigations on the effect of the fence geometry, in terms of δ/H , have also been included (Fang *et al.* 1997). Therefore, detailed discussions on the flow features are not intended in the present study.

In the problem of a steady flow past a two-dimensional, spring-supported, damped structure with a rectangular shape, as described by Blevins (1971), the amplitude of the lateral vibrations is highly affected by the reduced velocity and the damping ratio. When the fundamental frequency of the structure equals to the shedding frequency of the flow, the motion of the vibration becomes significant due to the occurrence of resonance. The resulting vibration amplitude decreases with an increase of the structure damping. On the other hand, as the flow speed increases so that the corresponding reduced velocity becomes large, flutter may occur if the structure damping cannot overcome the effect of the aerodynamic damping. In contrast, the present study illustrates an additional evidence of the effect of flow-induced vibration.

As the resulting wind load (drag) varies with time, it causes the elastic fence to vibrate. Within the range of the selected reduced velocities, the tip deflection is periodic and is symmetric to an equilibrium deflected position corresponding to that produced by the average wind load, as can be seen from the results in Figs. 6 and 7. The results in Figs. 7 also indicate that the modal damping ratio has no effect on the mean quantities of the tip response, which agrees with general concepts of structure dynamics.

The extent of the modal damping effect on the fluctuating quantities of the tip response, on the other hand, is different. Fig. 8a shows that there exist two peak values of A_r as U_r equals to 16.5 and 31, corresponding to the cases that the fundamental frequency of the fence is equal to either of the dominant frequencies of the flow. At these two resonance stages, the modal damping effect becomes significant. Similarly, large values of a_r are found as the fence becomes relatively soft ($U_r = 38$).

In the present case, the effect of the interaction (aerodynamic damping) is mainly induced by a change of surface load due to the structural motion relative to the wind speed. To investigate the extent of this effect, Fig. 9 illustrates the calculated spectra of C_D in several selected cases (no interaction and $U_r = 16.5, 31, 38$; $\zeta_{1,2} = 2\%$). The comparison shows that the resulting wind loads appear insensitive to the fence motions. Further examination on the tip motion histories in the case $U_r = 38$ and $\zeta_{1,2} = 2\%$ (Figs. 10) show that higher-mode response becomes excited, compared to those shown in Figs. 6. Additional evidence

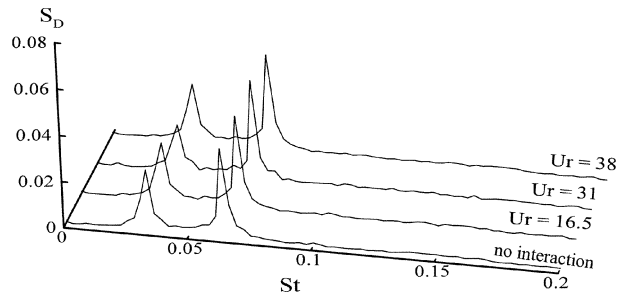


Fig. 9 Power spectra of drag coefficients

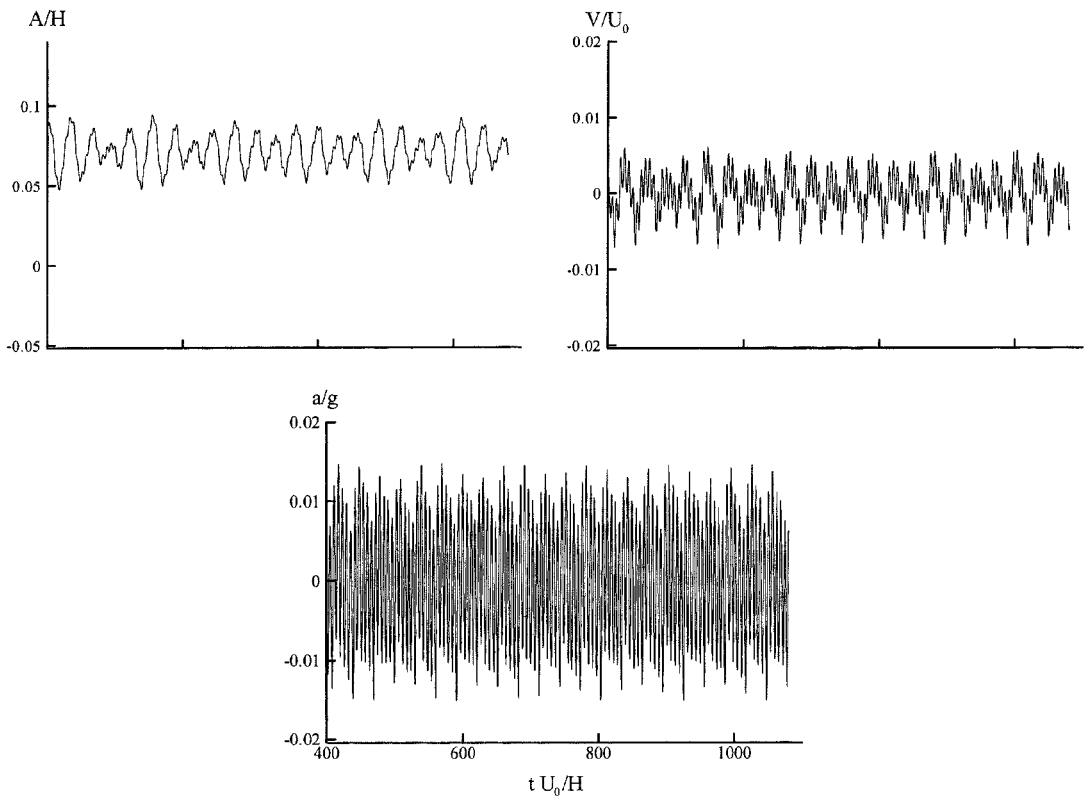


Fig. 10 Tip response histories ($U_r = 38$, $\zeta_{1,2} = 2\%$)

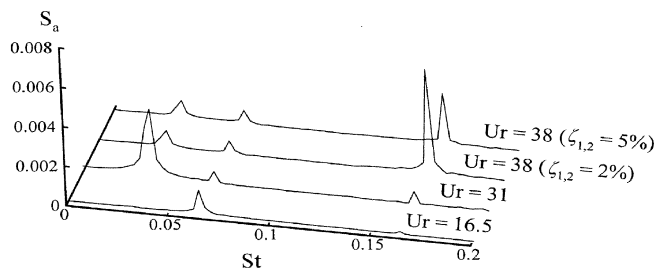


Fig. 11 Power spectra of tip acceleration

can also be found by comparing the spectra of the tip acceleration (see Fig. 11). In the case that $U_r=38$, besides the first two peaks associated with the occurrence of resonance, a third peak is detected at a Strouhal number corresponding to the second-mode frequency of the fence. Moreover, this peak becomes more significant in the case with a smaller value of modal damping. In contrast, excitation of second-mode response also occurs at resonance but the peak values are relatively small.

6. Conclusions

The unsteady turbulent flow around a surface-mounted elastic fence as well as the along-wind fence response was investigated numerically. By solving alternatively two sets of equations, one for the simulation of the unsteady turbulent flow and the other for the calculation of the dynamic motion of the fence, the mechanisms of the fence vibration under wind action were examined. The proposed numerical method is considered to be a useful tool for the analysis of problems involving flow-induced vibration. To be more practical, however, future developments of the numerical method should concentrate on the investigation of the effect of approaching flow characteristics (such as the unsteadiness and turbulence).

Based on the computational results, several conclusions are drawn as follows:

1. At a high Reynolds number, the flow around the fence is essentially unsteady and is dominated by two frequencies: one related to the shear layer vortices and the other one subject to vortex shedding. The resulting unsteady wind load causes the elastic fence to vibrate in the along-wind direction.
2. The tip deflection is periodic and is symmetric to an equilibrium deflected position, corresponding to the average wind load.
3. Modal damping has no effect on the mean tip response. However, it becomes important to the fluctuating response quantities, especially when resonance occurs or when the fence becomes relatively soft.
4. The root-mean-square values of the tip response can be enhanced under two situations: one is that when resonance occurs; the other one is that when the fence is relatively soft, which leads to excitation of higher-mode vibration.

Acknowledgements

The study was sponsored by a grant (NSC 81-0410-E-005-525) from the National Science Council in Taiwan. The computing time was provided by the National Center for High-Performance Computing in Taiwan.

References

- Blevins, R.D. (1971), *Flow-induced Vibration*, Van Nostrand Reinhold Company, New York, 5-10.
- Fang, Fuh-Min, Hsieh, W., Jong, S. and She, J. (1997), "Unsteady turbulent flow past solid fence", *J. Hydraulic Eng.*, ASCE, **123**(6), 560-565.
- Gupta, V.P. and Ranga-Raju, K.G. (1987), "Separated flow in lee of solid and porous fences", *J. Hydraulic Eng.*, ASCE, **113**(10), 1264-1276.
- Pearce, J.A., Qasim, A. Maxwell, T.T. and Parameswaran, S. (1992), "A computational study of coherent wake structures behind 2-D bluff bodies", *J. Wind Eng. Ind. Aerod.*, **41**, 2853-2861.
- Song, C. and Yuan, M. (1988), "A weakly compressible flow model and rapid convergence methods", *J. Fluids Eng.*, ASME, **110**(4), 441-455.
- Smagorinsky, J. (1963), "General circulation experiments with primitive equations", *Month Weather Rev.*, **91**(3), 99-164.